Research Article | Vol. 25, No. 24 | 27 Nov 2017 | OPTICS EXPRESS 29714
Optics EXPRESS

Efficient strategy to increase higher order inter-modal stability of a step index multimode fiber

AAMIR GULISTAN,* SOUVIK GHOSH, S. RAMACHANDRAN, AND B .M. A. RAHMAN

*aamir.gulistan@city.ac.uk

Abstract: We demonstrate a novel approach to enhance the mode stability through increased effective index difference (Δn_{eff}) between the higher-order modes (LP_{18}, LP_{09} and LP_{19}) of a multimode fiber. Fibers with large diameters have bigger effective mode areas (A_{eff}) and can be useful for high power lasers and amplifiers. However, a large mode area (LMA) results in an increased number of modes that can be more susceptible to mode coupling. The modal effective index difference (Δn_{eff}) strongly correlates with mode stability and this increases as the modal order (m) increases. We report here that the mode spacing between the higher order modes can be further enhanced by introducing doped concentric rings in the core. In our work, we have shown a more than 35% increase in the mode spacing between the higher order modes by optimizing the doping profile of a LMA fiber. The proposed design technique is also scalable and can be applied to improve the mode spacing between different higher order modes and their neighboring antisymmetric modes, as necessary.

OCIS codes: (060.2400) Fiber properties; (060.2310) Fiber optics; (230.2285) Fiber devices and optical amplifiers; (060.2280) Fiber design and fabrication.

References and links

1. D. J. Richardson, J. Nilsson, and W. A. Clarkson, "High power fiber lasers: current status and future perspectives," J. Opt. Soc. Am. B **27**, B63–B92 (2010).
2. M. N. Zervas and C. A. Codemard, "High power fiber lasers: A review," IEEE J. Sel. Top. Quantum Electron. **20**(5), 219–241 (2014).
3. J. W. Nicholson, J. M. Fini, A. M. DeSantolo, E. Monberg, F. DiMarcello, J. Fleming, C. Headley, D. J. DiGiovanni, S. Ghalmi, and S. Ramachandran, "A higher-order-mode Erbium-doped-fiber amplifier," Opt. Express **18**(17), 17651–17657 (2010).
4. J. S.Wong, W.Wong, S. Peng, J. McLaughlin, and L. Dong, "Robust single-mode propagation in optical fibers with record effective areas," CLEO-2005, CPDB10 (2005).
5. J. W. Nicholson, J. M. Fini, A. M. DeSantolo, X. Liu, K. Feder, P. S. Westbrook, V. R. Supradeepa, E. Monberg, F. DiMarcello, R. Ortiz, C. Headley, and D. J. DiGiovanni, "Scaling the effective area of higher-order-mode erbium-doped fiber amplifiers," Opt. Express **20**(22), 24575–24584 (2012).
6. S. Wielandy, "Implications of higher-order mode content in large mode area fibers with good beam quality," Opt. Express **15**(23), 15402–15409 (2007).
7. F. Stutzki, F. Jansen, H. J. Otto, C. Jauregui, J. Limpert, and A. Tunnermann, "Designing advanced very-large-mode-area fibers for power scaling of fiber-laser systems," Optica **1**(4), 233–242 (2014).
8. K. Rottwitt, S. M. M. Friis, M. A. U. Castaneda, E. N. Christensen and J. G. Koefoed, "Higher order mode optical fiber Raman amplifiers," 18th International Conference on Transparent Optical Networks (IEEE, 2016).
9. S. Ramachandran, J. W. Nicholson, S. Ghalmi, M. F. Yan, P. Wisk, E. Monberg, and F. V. Dimarcello, "Light propagation with ultralarge modal areas in optical fibers," Opt. Lett. **31**(12), 1797–1799 (2006).
10. J. M. Fini and S. Ramachandran, "Natural bend-distortion immunity of higher-order-mode large-mode-area fibers," Opt. Lett. **32**(7), 748–750 (2007).
11. A. Argyros, R. Lwin, and M. C. J. Large, "Bend loss in highly multimode fibres," Opt. Express **16**(23), 18590–18598 (2008).
12. S. Ramachandran, J. M. Fini, M. Mermelstein, J. W. Nicholson, S. Ghalmi, and M. F. Yan, "Ultra–large effective–area, higher–order mode fibers: a new strategy for high-power lasers," Laser Photon. Rev. **2**(6), 429–448 (2008).
13. A. W. Snyder and J. Love, *Optical Waveguide Theory* (Springer Science & Business Media, 1983).
14. B. M. A. Rahman and J. B. Davies, "Finite-element solution of integrated optical waveguides," J. Lightwave Technol. **2**(5), 682–688 (1984).

#301669 https://doi.org/10.1364/OE.25.029714
Journal © 2017 Received 1 Aug 2017; revised 26 Oct 2017; accepted 7 Nov 2017; published 14 Nov 2017

Optics EXPRESS

15. B. M. A. Rahman and J. B. Davies, "Penalty function improvement of waveguide solution by finite elements," in IEEE Trans. Microw. Theory Techn. **32**(8), 922–928 (1984).
16. S. Virally, N. Godbout, S. Lacroix, and L. Labonte, "Two-fold symmetric geometries for tailored phasematching in birefringent solid-core air-silica microstructured fibers," Opt. Express **18**(10), 10731–10741 (2010).
17. M. Koshiba and K. Inoue, "Simple and efficient finite–element analysis of microwave and optical waveguides," IEEE Trans. Microw. Theory Techn. **40**(2), 371–377 (1992).
18. V. Rastogi and K. S. Chiang, "Analysis of segmented-cladding fiber by the radial-effective-index method," J. Opt. Soc. Am. B **21**(2), 258–265 (2004).
19. A. Kumar, V. Rastogi, A. Agrawal, and B. M. A. Rahman, "Birefringence analysis of segmented cladding fiber," Appl. Opt. **51**(15), 3104–3108 (2012).
20. B. M. A. Rahman and J. B. Davies, "Vector–H finite element soluion of GaAs/GaAlAs rib waveguides," Proc. IEEE **132**(6), 349–353 (1985).
21. M. R. Karim, B. M. A. Rahman, and G. P. Agrawal. "Dispersion engineered $Ge_{11.5}As_{24}Se_{64.5}$ nanowire for supercontinuum generation: A parametric study," Opt. Express **22**(25), 31029–31040 (2014).
22. N. Lindlein, G. Leuchs, and S. Ramachandran, "Achieving Gaussian outputs from large-mode-area higher-order-mode fibers," Appl. Opt. **46**(22), 5147–5157 (2007).

1. Introduction

High power lasers and amplifiers are necessary for many applications in the field of science and technology. Recent research shows remarkable increase in the output power of fiber lasers [1, 2]. Compared to solid state lasers, fiber lasers are more compact, lightweight and flexible. Various approaches have been considered to increase the power of fiber based lasers and amplifiers. However, an increase in power brings the need to mitigate for non-linearities in the fiber such as Brillouin and Raman scattering, four-wave mixing (FWM) and self-phase modulation [3, 4]. Mitigating these non-linear effect require large mode area (LMA) fibers in which optical mode is less intense. Therefore, much of the recent research focuses on LMA fibers for the high-power fiber lasers [5]. Multimode fibers (MMF) offer large mode areas and high beam quality [6] but the existence of many modes can result in random mixing between the desired mode and unwanted modes. However, recent research shows that higher order modes (HOM) have the ability to provide for more stable operation because the signal stability increases with an increase in the modal order [5], [7, 8]. A number of approaches have been presented in recent years to use HOM for high power fiber lasers and amplifiers. One of the approaches involves the coupling of light from the fundamental mode to a single desired HOM using fiber Bragg gratings and then to propagate light in the higher order mode amplifying fiber [9]. These techniques provide considerably larger modal areas as well as more stable operation as described above. Moreover, for a given effective area, HOMs are also less sensitive to area reduction than the fundamental mode when bending [10, 11]. At the same time, compared to the fundamental mode, higher order modes are less prone to mode coupling as with the increase in the modal order (m) the difference in effective index (Δn_{eff}) between a given higher mode (LP_{0m}) and its nearest antisymmetric mode (LP_{1m}) also increases [12].

In this paper, we have proposed a novel approach to increase the Δn_{eff} that would result in a resilience to mode-mixing and more stable signal propagation with the advantage of significantly larger effective mode area (A_{eff}) by using HOMs. Annular rings with doping of increased or reduced refractive index are used at particular radial locations inside the core as shown in Fig. 1, such that the effective refractive index (n_{eff}) of a desired mode is increased or reduced [13]. To demonstrate our concept, we have considered a MMF of numerical aperture (NA=0.22) with core radius (R_{core}=25 μm) and refractive index (n_{core}=1.457). Similarly, cladding radius and refractive index are taken as (R_{clad}=62.5 μm) and (n_{clad}=1.4403), respectively. For this study the central operating wavelength of (λ=1.05 μm) is chosen.

Optics EXPRESS

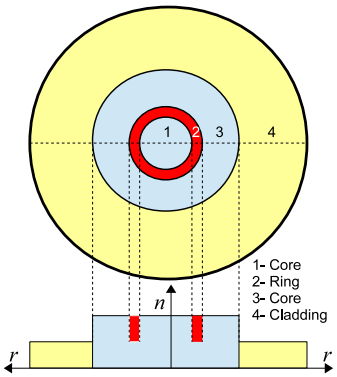

Fig. 1. Ring doping schematic of a MMF with the change in the refractive index along r-axis.

2. Theory

2.1. Modal solutions

Use of the higher order mode (HOM) of a multimode fiber (MMF) shows several advantages which includes mode area scaling to control laser high power and dispersion management for ultra-short pulses. Modal instabilities in HOMs are a common problem arising due to external perturbations, such as bending and fabrication imperfections. According to the symmetry rule, bend perturbation is odd in nature and direct coupling arises between even and odd order modes. Among the many modes guided by a MMF, sometimes a desired dominant mode (LP_{0m}) may transfer its energy to its nearest anti-symmetric ($LP_{1(m+1)}$ and $LP_{1(m-1)}$) modes on both sides [12]. A low effective index difference (Δn_{eff}) between adjacent modes enhances the modal energy transfer which results actual modal energy loss along with the interference effects. This could result in inter-mode mixing in a MMF. Although a lower order (lower value of m) mode may be easier to excite, a higher value of m gives larger modal separation (Δn_{eff}) values, so a compromise is needed. However, for a given value of m, if the modal separation to the nearest anti-symmetric modes can be increased, this would be a more preferable design. Here, a novel MMF design with several concentric material strips at strategically located positions is proposed to increase the Δn_{eff}=($n_{eff}^{0m} - n_{eff}^{1m}$) in desired modes, such as, LP_{18}, LP_{09} and LP_{19} as a high Δn_{eff} would restrict unwanted modal energy transfer due to external perturbations. Instead of using a perturbation approach, we have used a rigorous full vectorial **H**-field based finite element method (FEM) [14, 15] to find the modal solutions of our proposed MMF design. The FEM is one of the most numerically efficient and accurate approaches to obtain the modal solutions of an optical waveguide, to calculate the propagation constant (β), effective index (n_{eff}=β/k_o, where wavenumber k_o is given by $2\pi/\lambda$) and A_{eff}.

In order to increase the modal solution accuracy, the available two-fold symmetry of the fiber is exploited and only one-quarter of the structure is simulated [16, 17]. This allows more dense mesh distribution in the quarter structure of the fiber instead of distributing the same mesh over the whole structure. The polar mesh [18] discretization is also used, which can accommodate the discretized elements more efficiently at the circular boundaries, which can provide more accurate results compared to the mesh distribution based on the Cartesian coordinate system [19]. It is well known that the simulation accuracy of the FEM is highly dependent on the number of discretized elements used. Variation of the effective index (n_{eff}) with the number of mesh elements (N) is shown in Fig. 2 by a solid black line for the higher order LP_{09} mode. It can be observed that initially as mesh density increases the n_{eff} also increases rapidly and then asymptotically settles to a constant value. It should be noted that accuracy is up to the 3^{rd} decimal place when the

Optics EXPRESS

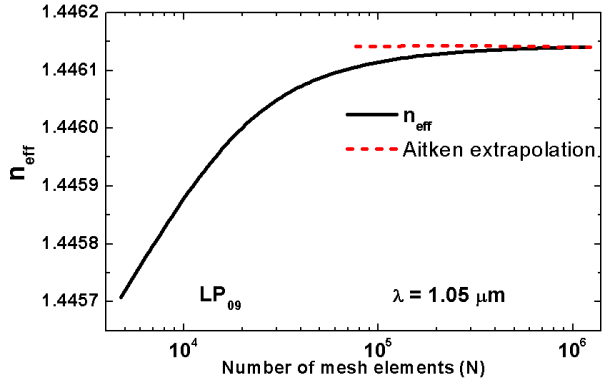

Fig. 2. Variation of $\mathbf{n}_{eff}$ of the LP_{09} mode with the mesh number (N) and convergence realized with the Aitken extrapolation technique.

number of elements used is, N=7×10^4 and it increases to the 5^{th} decimal place when N=5 × 10^5. Here N, is the number of triangular elements used to represent a quarter of the MMF. A powerful Aitken's extrapolation technique is used to test the convergence of the modal solutions [20, 21]. Three successive n_{eff} values for corresponding mesh divisions with a geometric ratio are used in the Eq. (1).

$$n_{\text{eff}}^{\infty} = n_{\text{eff(r+1)}} - \frac{[n_{\text{eff(r+1)}} - n_{\text{eff(r)}}]^2}{n_{\text{eff(r+1)}} - 2n_{\text{eff(r)}} + n_{\text{eff(r-1)}}} \tag{1}$$

Using Eq.1 the extrapolated values of n_{eff}^{∞} are shown in the Fig.2 by the red-dashed line. Aitken's values are calculated for the mesh values N=7.66 × 10^4, 3.07 × 10^5, and 1.23 × 10^6 increased in fixed geometric ratio yielding the n_{eff} values 1.4460355, 1.4461157,and 1.4461358, respectively. It should be noted that in each solution the mesh density is two times (no. of the elements is four times) that of the previous and thus the geometrical mesh ratio is kept constant. From these values a more accurate extrapolated value of 1.4461398 is obtained. Similarly, Fig. 2 clearly shows the convergence of the extrapolated results and raw FEM results. As the trend of n_{eff} with increasing N for different modes is similar, so the accuracy of Δn_{eff} between two modes with increasing N is also greater.

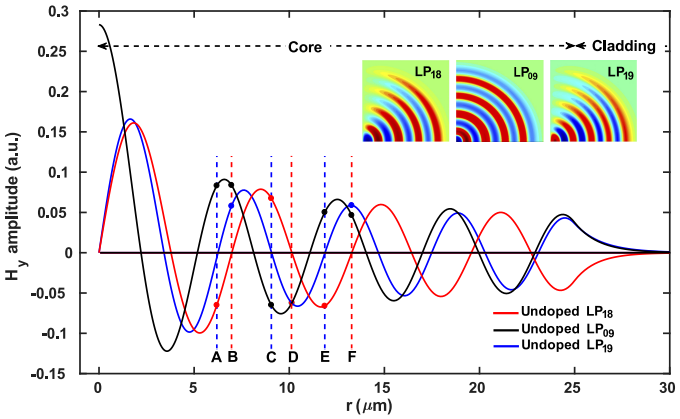

Fig. 3. Variations of H_y fields of the LP_{18}, LP_{09}, and LP_{19} modes along the r-axis of MMF, contour field profiles in inset and the key points of interest are also shown.

Optics EXPRESS

2.2. Mode stability

As previously discussed, higher order modes (HOM) provide the unique benefit of increased stability due to a greater mode spacing (Δn_{eff}) compared with that of the fundamental modes (LP_{01}) [22]. In this paper, we propose a unique approach that can reduce mode mixing between the higher order LP_{18}, LP_{09} and LP_{19} modes, that could alternatively only be possible by considering a much higher modal order. For our design, we used LP_{09} as the central propagation mode and modified the refractive index profile of the fiber such that the mode stability between symmetric (LP_{09}) and the two nearest antisymmetric (LP_{18} and LP_{19}) modes is increased. A measure of the modal stability can be defined using the effective index differences as, S_1=$\Delta n_{eff}(LP_{18} - LP_{09})$ and S_2=$\Delta n_{eff}(LP_{09} - LP_{19})$. However, if required any other HOM of interest can also be selected and using the same concept its mode stability can be enhanced. For this structure, the effective indices of the LP_{18}, LP_{09}, and LP_{19} are calculated as 1.447317, 1.4461104, and 1.4448554, respectively, yielding S_1=0.0012066 and S_2=0.001255. The variation of the dominant H_y field profile of the LP_{18}, LP_{09} and LP_{19} modes is shown in Fig. 3 by red, black and blue lines, respectively. H_y field contours of the LP_{18}, LP_{09} and LP_{19} modes are also shown Fig. 3 as insets. It can be observed that the field profile of LP_{09} shown by a black line, has the highest magnitude at the center (r=0) of the fiber and eight zero values along the radial direction. The antisymmetric LP_{18} and LP_{19} modes shown with red and blue lines, respectively, have zero field values at the center (r = 0) of the fiber. The dominant H_y fields of the LP_{18} and LP_{19} modes have eight and nine zero field values along the radial direction, respectively. Table 1 shows all the radial locations where these modes have zero field values. For example, LP_{18} has its first three zero field locations at r=0, 3.78 and 6.966 μm. Using these zero crossings we have identified multiple locations that are suitable for doping such that the mode stability (S_1 and S_2) can be increased.

Table 1. Zero crossing locations of field profiles of the LP_{18}, LP_{09} and LP_{19} modes along r-axis (μm).

Mode	Location of zero crossings along r-axis (μm)							
LP_{18}	0	3.78	6.966	10.138	13.279	16.315	19.557	22.684
LP_{09}	2.16	5.16	8.125	11.078	13.99	16.89	19.9	22.79
LP_{19}	0	3.36	6.193	9.058	11.867	14.577	17.472	20.252

Some specific points, A, B, C, D, E and F are selected as shown in Fig. 3, where either LP_{18} or LP_{19} has zero crossing. The reason for choosing these points is that we want to have less of an effect on one of the mode and have more of an effect on the other two though using strips of different doping. The modal field values at these points are also given in Table 2. For example at

Table 2. Field values of LP_{18}, LP_{09} and LP_{19} at A, B, C, D, E and F points.

Mode	A=6.193	B=6.966	C=9.058	D=10.138	E=11.867	F=13.279
LP_{18}	0.06507	0	0.06741	0	0.6606	0
LP_{09}	0.08321	0.08328	0.06493	0.06218	0.05022	0.04658
LP_{19}	0	0.058	0	0.06267	0	0.05879

point A, the H_y field value of LP_{19} is zero, whereas, the field values of LP_{18} and LP_{09} modes are 0.06507 and 0.08321, respectively. As a result any change of refractive index doping at point A will have an almost negligible effect on the LP_{19} mode and comparatively more of an effect on the LP_{09} than the LP_{18} mode. However, at point F, where the H_y field value of LP_{18} mode is zero and these values for LP_{09} and LP_{19} modes are 0.04658 and 0.05879, respectively. Hence, at point F, doping will have no effect on the LP_{18} but will have more of an effect on LP_{19} than the

Optics EXPRESS

LP_{09} mode. This will result in an increase in effective index both of these modes while keeping the effective index of the LP_{18} mode unchanged, and a suitable selection can result in an increase in the modal stability. In order to increase the Δn_{eff} between these modes a circular strip of 0.3 μm width is considered that can have an increased or reduced refractive index by Δn. Here, we have taken Δn=0.0167, which is also the difference between the core and cladding refractive indices. However, different values of Δn in these strips can be chosen according to the required level of stability between modes.

3. Numerical results

Table 3 shows the effect of doping a single individual layer at the above mentioned six positions along the r-axis. The second column of Table 3 shows the original Δn_{eff} between the modes without any doping. It can be noted that the Δn_{eff} between LP_{09} and LP_{19} is slightly higher than the Δn_{eff} between LP_{18} and LP_{09}. The values of $+\Delta n$ or $-\Delta n$ on particular points are chosen such that the effect on the central mode, in our case LP_{09}, is negligible or can be compensated with another doping layer where Δn is chosen with an opposite sign to the first point. For example, in layer A (at r=6.193 μm), $+\Delta n$ is chosen to increase the stability, S_1 between LP_{09} and LP_{19}, but unfortunately this reduces the stability, S_2 between LP_{18} and LP_{09}. On the other hand a reduction of refractive index in layer B increases modal separation S_2, but reduces that of S_1. However, an increase of refractive index in layer E and reduction in layer F enhances both the S_1 and S_2 modal stabilities. The same doping approach is considered at all six positions with either $+\Delta n$ or $-\Delta n$ as shown in Table 3. Here, two approaches can be considered;

1. Using single layer doping to increase the stability between modes.
2. Using the combination of two or more layers to increase the stability.

Table 3. Individual strip doping effect on Δn_{eff} at points A, B, C, D, E, and F.

Δn_{eff}	Without doping	A	B	C	D	E	F
		+Δn	-Δn	+Δn	-Δn	+Δn	-Δn
$S_1 = LP_{18}$-LP_{09}	0.0012066	0.0010515	0.0015574	0.0012192	0.0014932	0.0013553	0.0014033
$S_2 = LP_{09}$-LP_{19}	0.001255	0.0015544	0.0010634	0.0015037	0.0012711	0.0014385	0.0014217

In Table 4 the above described approaches are shown with the percentage increase in Δn_{eff} (S_1 and S_2). The percentage increase is calculated with respect to the original Δn_{eff} between the modes as shown in column two. Here, three different options are suggested depending upon the required increase in the Δn_{eff}. It can be seen that with a single layer of $-\Delta n$ doping at point F, S_1 and S_2 are increased by 16% and 14%, respectively. However, using two layers (at E & F points) the stabilities S_1 and S_2 between modes can be increased by 20% and 23%, respectively. It should be noted that the Δn doping at points E and F are taken as positive and negative, respectively. For further enhancement, three layers can be doped simultaneously at points C, D, and E which results in an increase of 35% and 38% for $\Delta n_{eff}(LP_{18} - LP_{09})$ and $\Delta n_{eff}(LP_{09} - LP_{19})$, respectively. Hence, our proposed design results in increased modal spacing between the higher order modes LP_{18}, LP_{09} and LP_{19}, thus providing for more stable and mode-mixing resistant operation. Figure 4 shows the refractive index profile for three layer doping at C, D and E points. Here, Δn at points C and E are taken as positive such that it increases the local refractive index from 1.457 to 1.4737. Whereas, at point D, Δn is taken as negative resulting in the local index being equal to that of the cladding. The combination is chosen such that $\Delta n_{eff}(LP_{18} - LP_{09})$ and $\Delta n_{eff}(LP_{09} - LP_{19})$ have an almost equal increase. Here, all three annular strips are centered at points C, D and E and have an equal width of 0.3 μm. The LP_{09} mode is considered as a central

Optics EXPRESS

Table 4. Percentage increase in the Δn_{eff} using individual and combination approach.

Δn_{eff}	Without doping	F only		E & F		C, D & E	
		Δn_{eff}	% Increase	Δn_{eff}	% Increase	Δn_{eff}	% Increase
$S_1 = LP_{18}$-LP_{09}	0.0012066	0.0014033	16	0.0014551	20	0.0016254	35
$S_2 = LP_{09}$-LP_{19}	0.001255	0.0014217	14	0.0015318	23	0.0017357	38

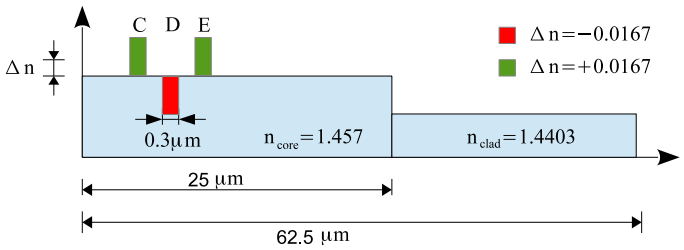

Fig. 4. Refractive index profile of the modified MMF along r- axis with ±Δn at C, D and E points.

propagation mode in our design. Hence next, the effect of three layers of doping at points C, D, and E points on the field profile of LP_{09} is studied. Figure 5 shows the H_y field profile of the LP_{09} mode before and after doping. The black line shows the undoped field profile whereas the dotted blue line represents the field profile of LP_{09} after doping these three layers at C, D, and E. It can be observed that until the appearance of the doped strips the field profile was almost unchanged, however beyond these strips, the field value is reduced compared to that of the original undoped fiber.

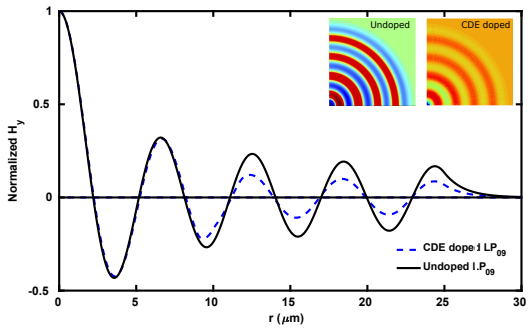

Fig. 5. Variations in the H_y fields of LP_{09} modes along the r-axis of the undoped fiber and the fiber with C, D, and E layers doped. The contour field profiles are also shown inset.

The Δn=0.0167 value used for the circular strips C, D, and E is equivalent to the refractive index difference between core and cladding of the fiber but of necessary other Δn values or even unequal values can be used for a particular design. To observe the effect of increased or reduced value of Δn, we have halved the refractive index difference as, ±Δn=0.00835 and found that the modal stabilities S_1 and S_2 reduces to 18% and 19%, respectively. However, when refractive index difference is increased to double; as ±Δn=0.0334, the modal stabilities S_2 increases to 74% but S_1 increased only slightly to 41%, as field profiles were distorted significantly. However, it can be stated that a significant enhancement in the modal stability can be achieved by this approach.

Although we have focused on the enhancement of mode spacing between LP_{09} and its neighboring antisymmetric LP_{18} and LP_{19} modes, however, our approach is scalable and can be

Optics EXPRESS

applied for any higher order modes. As an example, for the enhancement of mode spacing of LP_{08} mode and its neighboring antisymmetric LP_{17} and LP_{18} modes, we have carried out additional simulations after introducing the similar annular rings. Similar six zero crossing points, $A^{'}$ to $F^{'}$ for LP_{17} or LP_{18} are identified as $A^{'}$=6.928, $B^{'}$=7.856, $C^{'}$=10.138, $D^{'}$=11.518, $E^{'}$=13.279, $F^{'}$=15.098 (in μm). Numerical simulations were carried out with strips width of 0.3 μm and $\pm\Delta n$=0.0167 introduced at these points. Table 5 shows the increase in $\Delta n_{eff}(LP_{17} - LP_{08})$ and $\Delta n_{eff}(LP_{08} - LP_{18})$ with single layer ($F^{'}$) or multiple layers ($E^{'}$, $F^{'}$ and ($C^{'}$, $D^{'}$, $E^{'}$) with perturbed annular strips. It can be observed that the stability is increased to 46% for the LP_{08} mode when three annular layers at ($C^{'}$, $D^{'}$, $E^{'}$) points are used. This confirms that the concept presented here can be applied to any higher order modes, as necessary.

Table 5. Percentage increase in the Δn_{eff} of LP_{08} mode and its neighboring antisymmetric modes using individual and combination of two or three strips doping.

Δn_{eff}	Without doping	$F^{'}$ only		$E^{'}$ & $F^{'}$		$C^{'}$,$D^{'}$ & $E^{'}$	
		Δn_{eff}	% Increase	Δn_{eff}	% Increase	Δn_{eff}	% Increase
LP_{17}-LP_{08}	0.0010746	0.0012218	14	0.0013424	25	0.0015759	47
LP_{08}-LP_{18}	0.0011146	0.0013136	18	0.0015187	36	0.0016256	46

3.1. Fabrication tolerance of strips width

Here, we demonstrate the effect of possible variations in doping that can occur during the fabrication process. As the combined doping of the three layers at points C, D, and E could be more sensitive to fabrication tolerances than the two or single layer doping we will consider the three layers (C, D and E) case for further investigation. The effects of a change in the layer width (w) from 0.3 μm to a higher or lower value are shown in Fig. 6. As discussed earlier, with w=0.3 μm the stabilities S_1 and S_2 between the modes are 35% and 38%, respectively. With an increase in the width from w=0.3 μm to w=0.4 μm, the stabilities S_1 and S_2 further increase to 38% and 51%, respectively. This is because the area of the doped layer is increased when the width is changed from 0.3 μm to 0.4 μm thus increasing its overall effect. However, as the width deceases to w=0.20 μm, the stability improvement reduces but still it remains above 25%. Hence, in our proposed design the modal stability improvement will remain at least 25% larger for a width change of $\pm$0.1 μm.

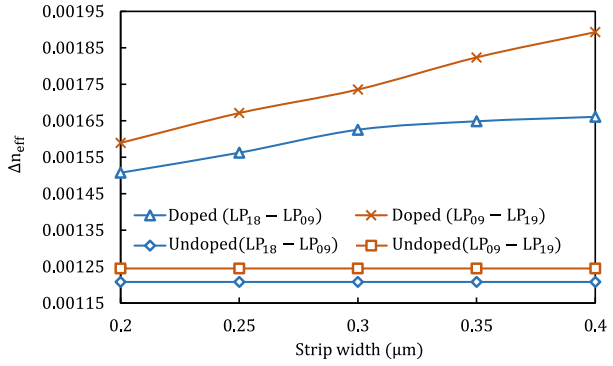

Fig. 6. Effect on Δn_{eff} of a change in width of doped layers at points C, D, and E.

Optics EXPRESS

3.2. Fabrication tolerance of strips center location

In our proposed design three layers are centered at points C=9.058 μm, D=10.138 μm and E=11.867 μm and during fiber drawing these positions may change. Figure 7 shows the effect of a change in the location of the doped layer's center points. It can be seen that the stability is highly dependent on the specified locations in Fig. 3. When there is no shift in the location of the strip's centers, the stability improvement is larger than 35%. With a tolerance of $\pm 0.05 \mu m$ the stability improvement still remains above 27% but as the shift is increased to $0.1 \mu m$ the S_1 improvement drops to 20% while S_2 improvement is increased to 51%. Moreover, when the annular strips shift is -0.1 μm, the modal stability S_1 improvment increases to 46% but that of S_2 decreases to 27%. For comparison the spacing between the modes before introduction of the C, D and E layers is also shown by two horizontal lines.

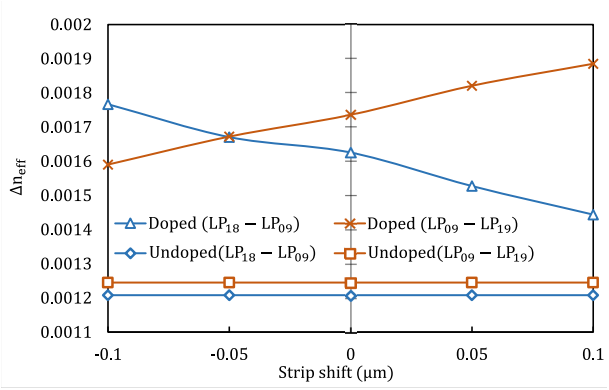

Fig. 7. Effect on the Δn_{eff} of a variation in the position of C, D, and E layers from center location.

3.3. Fabrication tolerance of wavelength change

The above analysis is carried out at the center wavelength of λ=1.05 μm. However, when the operating wavelength changes from this value the stability between modes can also change. To observe the impact of wavelength change on the stability between the modes, we varied the operating wavelengths and this is shown in Fig. 8. It can be observed that the stability between the LP_{18}, LP_{09} and LP_{19} modes increases with an increase in the wavelength. It should be noted that the refractive index of a material is also dependent on the wavelength. In our analyses we have used the core and clad refractive index values as n_{core}=1.457 and n_{clad}=1.4403 respectively at λ=1.05 μm. However, if required the effect of refractive index variation with the wavelength can also be included. It should be noted that without doping at the C, D, and E layers, the stability increases almost linearly with an increase in the wavelength. The increased wavelength reduces mode confinement and effective index values and this also increases the separation between the modal index values. A similar effect is noticed after the introduction of doping at layers C, D and E layers. When the center wavelength is λ=1.05 μm, the modal stability values are S_1=0.0016254 and S_2=0.0017357, which are improvements of 35% and 38% from their undoped values, respectively. However, it can be noted that with a change in the wavelength from λ=1.05 μm to λ=0.85 μm the stability difference after doping shows a similar trend to the undoped case. The modal stability values at λ=0.85 μm reduced to S_1=0.0010095 and S_2=0.0014572, however this reflects a 25% and 74%, improvement from the standard fiber. Similar behavior is observed when the center wavelength is increased to λ=1.25 μm and modal stability increases to S_1=0.002199 and S_2=0.0019263, and these reflect improvements 35% and 25% increase from the standard fiber. The modal stability still remains 25% higher for the wavelength range from λ=0.85

Optics EXPRESS

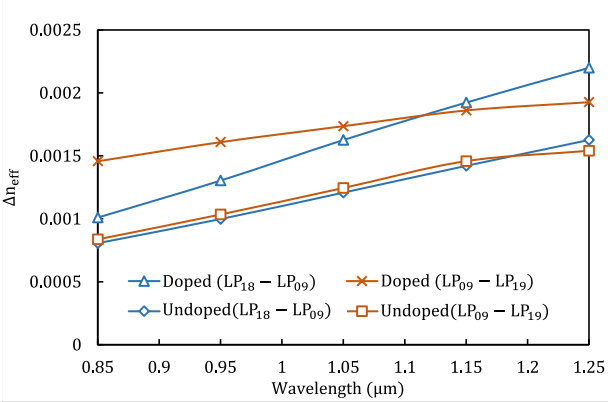

Fig. 8. Effect on the Δn_{eff} with the change in wavelength (λ)

μm to λ=1.25 μm, and hence the proposed design results in a sufficiently improved stability between the competing modes and is also expected to provide for large effective mode areas A_{eff} because of operating in HOMs [12].

4. Conclusions

We have proposed a novel design approach, which has been validated by rigorous numerical analysis, to improve the stability between the modes can be increased by more than 35%. Increasing the Δn_{eff} between modes results in a more stable and mode-mixing resistant operation and thus allows scalability of power in laser applications. It is also shown here that the design is reasonably stable to possible fabrication tolerance such as the position and width of the doped annular sections.